Eur. Phys. J. D **28**, 49–57 (2004)
DOI: 10.1140/epjd/e2003-00283-5

THE EUROPEAN PHYSICAL JOURNAL D

Analysis of the hot band of stannane $^{116}SnH_4$ in the 600–850 cm^{-1} range

A. Tabyaoui[1,2,a], G. Pierre[3], and H. Bürger[4]

[1] FST Settat, km 3, B.P. 577, 26000 Settat, Morocco
[2] LETS, Faculté des sciences, avenue Ibn Batouta, B.P. 1014, Rabat, Morocco
[3] LPUB, CNRS UMR 5027, Faculté des sciences Mirande, 9 rue Alain Savary, B.P. 47870, 21078 Dijon, France
[4] Anorganische Chemie, FB 9, Universität-GH, Gauss-Str. 20, 5600 Wuppertal 1, Germany

Received 16 July 2003 / Received in final form 7 August 2003
Published online 8 October (2003) –

Abstract. The FTIR spectrum of monoisotopic stannane $^{116}SnH_4$ has been recorded in the 600–850 cm^{-1} range, with the Bruker 120 HR interferometer at Giessen, Germany. The resolution was 2.1×10^{-3} cm^{-1}. The analysis of infrared transitions in this region enabled Brunet *et al.* [1] to assign many lines to the bending dyad ν_2/ν_4. However, several lines in this spectrum were found to be unassigned. In a recent work [2], we have analysed the infrared spectrum of stannane in the bending triad region at 1400 cm^{-1}. The results obtained enabled us to assign directly, for the spectrum in the region 600–850 cm^{-1}, 163 of the observed transitions to the hot band {bending triad} minus {bending dyad} up to $J = 9$. These transitions were combined to the infrared data corresponding to the bending triad $(2\nu_2, \nu_2 + \nu_4, 2\nu_4)$, to refine a set of Hamiltonian parameters for the two bands $2\nu_2$ and $(\nu_2 + \nu_4)$ [2].

PACS. 33.20.Vq Vibration-rotation analysis – 33.20.Ea Infrared spectra

1 Introduction

Many experimental and theoretical studies were devoted to tetrahedral molecules generally and to the stannane molecule SnH_4 particularly, using Raman, infrared and microwave spectroscopy. The first work on stannane was done by Levin and Ziffer [3] who determined some molecular constants and showed that the two bending modes $\nu_2(E)$ and $\nu_4(F_2)$ are strongly coupled by a first order Coriolis interaction. Kattenberg and Oskam [4] measured the four fundamental bands $(\nu_1(A_1), \nu_2(E), \nu_3(F_2), \nu_4(F_2))$ using Raman and infrared spectroscopy and found that the infrared inactive ν_1 band was only 2.5 cm^{-1} above the infrared active ν_3 band. Thereafter, Birss [5] showed that the ν_1 and the ν_3 vibrational states are coupled by a second order rotation-vibration interaction term. Generally this interaction is not strong but becomes very important when the wavenumber difference of the two bands is within a few cm^{-1}. In the infrared, the formally forbidden ν_1 transitions can therefore borrow intensity from the allowed ν_3 transitions and be observed. Such interactions have been observed in SiH_4 [6] and GeH_4 [7].

It is well-known that tetrahedral molecules, which are non polar in their equilibrium configuration, develop a small induced dipole moment by excitation of a triply degenerate vibration [8,9]. Pure rotational transitions resulting from this induced dipole moment have been observed for several tetrahedral molecules [10–16].

Jörissen *et al.* [17] have recorded and analysed the infrared spectrum of the (ν_1/ν_3) dyad of stannane in natural isotopic abundance. Their technique used infrared-microwave double resonance employing a tunable diode laser. They have determined for each of the five most abundant isotopic species of stannane seventeen constants by fitting simultaneously the infrared and microwave data using for the ground state and the $\nu_1 = 1$ state the Hamiltonian of Kirschner and Watson [18] and for the $\nu_3 = 1$ state that of Robiette *et al.* [19]. Only one coupling term between ν_1 and ν_3 given by Cabana *et al.* [6] and expressed by Susskind [20] in a tensorial form as $\mathbf{H}(\nu_1/\nu_3) = d_{13}\mathbf{T}_{123}$ was used. The ground state parameters used in their fit were those determined by Ohshima *et al.* [21,22].

Krivtsun *et al.* [23] recorded and analysed the FTIR spectrum of monoisotopic stannane $^{120}SnH_4$ in the 1903–1960 cm^{-1} region. More than 230 transitions of the $^{120}SnH_4$ isotopic specie were used for simultaneous analysis of the ν_1, ν_3 resonance states. They have determined 21 spectroscopic parameters of the upper states using a model Hamiltonian developed to the forth order

[a] e-mail: atabyaoui@yahoo.fr

of approximation, which explicitly takes into account the resonance interaction.

The (ν_1/ν_3) stretching dyad of stannane was reinvestigated by Tabyaoui *et al.* [24,25] near 1900 cm^{-1}, employing a monoisotopic sample, $^{116}SnH_4$, by which ambiguities caused by mutual blending of lines, belonging to different isotopic species could be circumvented. They have recorded and analysed the FTIR and high-resolution Stimulated Raman spectra. A simultaneous analysis of the Raman, infrared and microwave data using a Hamiltonian developed to the sixth order for the (ν_1/ν_3) dyad enabled them to determine 4 parameters for the ν_1 band, 17 parameters for the ν_3 band and 6 interaction parameters. The line transitions were assigned up to $J = 14$. They have shown that for high J values ($J > 14$), a perturbation appears due to an interaction between the stretching dyad (ν_1/ν_3) and the second overtone of bending modes $(3\nu_2, 2\nu_2 + \nu_4, \nu_2 + 2\nu_4, 3\nu_4)$. In the fit of the Hamiltonian parameters, the ground state parameters were fixed to the values determined by Brunet *et al.* [1], where the tensorial ones are close to the values determined by Ohshima *et al.* [21,22].

$^{116}SnH_4$ was investigated too by Brunet *et al.* [1] who analysed the FTIR spectrum of the (ν_2/ν_4) dyad using a sixth order Hamiltonian. The analysis of the infrared transitions allowed them to determine 10 ground state parameters, $9\nu_2$ parameters, $17\nu_4$ parameters and 18 interaction parameters.

Halonen *et al.* [26] have analysed the FTIR spectrum of the (2000, A_1/F_2) stretching vibrational band system of $^{116}SnH_4$ up to $J = 20$ and refined 21 Hamiltonian parameters in a local mode model. Also, Halonen *et al.* [27] have analysed the FTIR spectra of the (1000, A_1/F_2), (2000, A_1/F_2), (3000, A_1/F_2) vibrational band systems for $^{120}SnD_4$. They have made a rotational analysis of the spectra. The local mode relations obtained confirm that vibrational energy localization takes place in the second stretching vibrational overtone of deuterated stannane.

Recently, we have made an analysis of the FTIR spectrum of the monoisotopic stannane in the 1400 cm^{-1} region corresponding to the bending triad [2]. The results obtained enabled us to assign directly most observed transitions to the hot band {bending triad} minus {bending dyad} near 700 cm^{-1}. We have then included these transitions in the fit of the Hamiltonian parameters. The simultaneous analysis of infrared data corresponding to both hot band and bending triad enabled us to determine 26 Hamiltonian parameters for the $2\nu_2$ and $(\nu_2 + \nu_4)$ bands [2]. The standard deviation was 1.5×10^{-3} cm^{-1}.

In this work, we present for the hot band {bending triad} minus {bending dyad}, the assignments realized up to $J = 9$ and the results obtained for this hot band during the analysis of the bending triad $(2\nu_2, \nu_2 + \nu_4, 2\nu_4)$.

2 Experimental details

Monoisotopic stannane, $^{116}SnH_4$, was prepared by reacting a solution containing $SnCl_6^{2-}$ (1 mg Sn/ml), obtained by dissolving ^{116}Sn (98% ^{116}Sn, Oak Ridge) in an aqueous HCl/HNO_3 mixture, with an aqueous solution of $NaBH_4$ (3%) in vacuum (50–80 mbar). Gaseous $^{116}SnH_4$ evolved was collected at −196 °C and purified by repeated fractional condensation using a standard vacuum line, yield ∼90%.

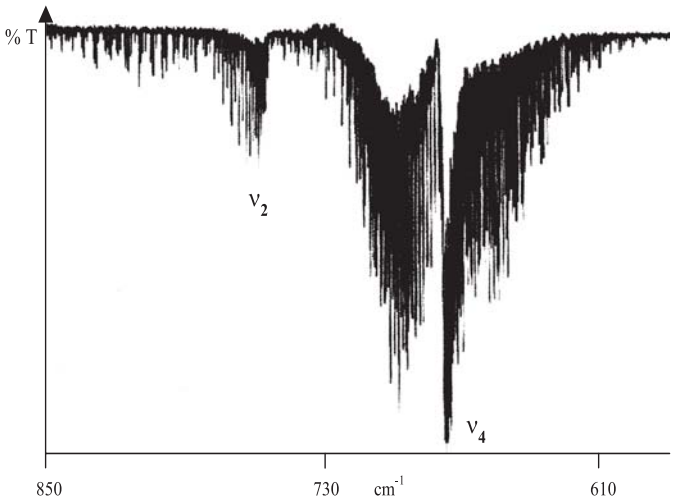

Fig. 1. Experimental spectrum of monoisotopic stannane $^{116}SnH_4$.

FTIR spectra were recorded at Giessen in the 490–980 cm^{-1} range with a Bruker 120 HR spectrometer equipped with a Ge/KBr beam splitter and a Cu:Ge detector. The resolution, trapezoidal apodization, was 2.0×10^{-3} cm^{-1}; the Doppler width at 700 cm^{-1} is approx. 0.7×10^{-3} cm^{-1}. The actual width of weak lines (FWHM) was $\sim2.1\times10^{-3}$ cm^{-1}. A cell of 18.7 cm length equipped with KBr windows was employed, and a pressure of 1 mbar chosen. A total of 50 scans were co added. Calibration was performed with N_2O lines [28]; relative to these lines it is better than 1.0×10^{-4} cm^{-1}.

The medium-resolution spectrum showed in Figure 1 was recorded with a Nicolet 7199 FTIR spectrometer employing a resolution of 0.05 cm^{-1}.

3 Theory

The transformed vibrational-rotational Hamiltonian for tetrahedral molecules developed by Champion and Pierre [29–31] is especially well adapted for vibrational extrapolation. Vibrational operators are expressed in terms of tensor products of creation and annihilation elementary operators in such a way that each term of the Hamiltonian expansion corresponds to a given vibrational state or set of quasi-degenerate vibrational states. According to this scheme, the completely transformed Hamiltonian for the vibrational states taken into account in this work, can be written as

$$\widetilde{\mathbf{H}} = \widetilde{\mathbf{H}}_{\{GS\}} + \sum_s \widetilde{\mathbf{H}}_{\{\nu_s\}} + \sum_s \widetilde{\mathbf{H}}_{\{2\nu_s\}} + \sum_{s<s'} \widetilde{\mathbf{H}}_{\{\nu_s+\nu_{s'}\}}. \quad (1)$$

In this expansion, $\widetilde{\mathbf{H}}_{\{GS\}}$ contains only pure rotational operators of the type J^{Ω} (J designating one component J_x, J_y or J_z of the angular-momentum operator). In the notation introduced in [29–31] its tensorial expression is

$$\widetilde{\mathbf{H}}_{\{GS\}} = \sum \mathbf{t}_0^{\Omega(K,A_1)}\, \mathbf{T}_0^{\Omega(K,A_1)}. \tag{2}$$

$\widetilde{\mathbf{H}}_{\{\nu_s\}}$ gathers all terms of type $r_s^2 J^{\Omega}$ (r_s designating q_s or p_s) quadratic in the ν_s mode elementary operators. Its tensorial expression [29–31] is

$$\widetilde{\mathbf{H}}_{\{\nu_s\}} = \sum \mathbf{t}_{s,s}^{\Omega(K,\Gamma)}\, \mathbf{T}_{s,s}^{\Omega(K,\Gamma)}. \tag{3}$$

$\widetilde{\mathbf{H}}_{\{\nu_s+\nu_{s'}\}}$ gathers all term quartic in the ν_s and $\nu_{s'}$ mode elementary operators of the type $r_s^2 r_{s'}^2 J^{\Omega}$. Its tensorial expression [29–31] is

$$\widetilde{\mathbf{H}}_{\{\nu_s+\nu_{s'}\}} = \sum \mathbf{t}_{ss',ss'}^{\Omega(K,\Gamma)\Gamma_1\Gamma_2}\, \mathbf{T}_{ss',ss'}^{\Omega(K,\Gamma)\Gamma_1\Gamma_2}. \tag{4}$$

The expression for $\widetilde{\mathbf{H}}_{\{2\nu_s\}}$ is quite similar and can be obtained by setting $s' = s$ in (4).

In the above expressions and throughout this paper, $\mathbf{T}_{s\ldots,s'\ldots}^{\Omega(K,\Gamma)\Gamma_1\Gamma_2}$ is a rovibrational operator obtained by coupling rotational and vibrational operators:

$$\mathbf{T}_{s\ldots,s'\ldots}^{\Omega(K,\Gamma)\Gamma_1\Gamma_2} = \beta_{\Omega K}^{\Gamma_1} \left(\mathbf{R}^{\Omega(K,\Gamma)} \times \mathbf{V}_{s\ldots,s'\ldots}^{\Gamma_1\Gamma_2(\Gamma)}\right)^{(A_1)} \tag{5}$$

where

$$\begin{aligned} \beta_{\Omega K}^{\Gamma_1} &= 1 && \text{if } K \neq 0 \\ &= [\Gamma_1]^{1/2} \left(\frac{-3^{1/2}}{4}\right)^{\Omega/2} && \text{if } K = 0. \end{aligned}$$

The rotational operator is denoted by $\mathbf{R}^{\Omega(K,\Gamma)}$ where Ω, K and Γ designate respectively rotational degree, tensor rank in the rotation group $O(3)$, and symmetry in the group T_d. It is obtained by tensorial coupling of Ω elementary rotational operators, and the vibrational operator $\mathbf{V}_{s\ldots,s'\ldots}^{\Gamma_1\Gamma_2(\Gamma)}$ is obtained by tensorial coupling of $s\ldots$ elementary creation operators and of $s'\ldots$ elementary annihilation operators. The value of $[\Gamma_1]$ is the dimension of the representation. Details of the coupling of different operators can be obtained in [31].

The rovibrational effective Hamiltonian for a set of interacting states $\langle\nu\rangle$ is given by:

$$\mathbf{H}^{\langle\nu\rangle} = \mathbf{P}^{\langle\nu\rangle}\widetilde{\mathbf{H}}\mathbf{P}^{\langle\nu\rangle} \tag{6}$$

where $\mathbf{P}^{\langle\nu\rangle}$ is the projector operator on the vibrational Hilbert subspace.

The ground-state effective Hamiltonian contains terms from $\widetilde{\mathbf{H}}_{\{GS\}}$ only:

$$\begin{aligned} \mathbf{H}^{\langle GS\rangle} &= \mathbf{P}^{\langle GS\rangle}\widetilde{\mathbf{H}}_{\{GS\}}\mathbf{P}^{\langle GS\rangle} \\ &= \sum \mathbf{t}_0^{\Omega(K,A_1)}\mathbf{P}^{\langle GS\rangle}\mathbf{T}_0^{\Omega(K,A_1)}\mathbf{P}^{\langle GS\rangle} \end{aligned} \tag{7}$$

where $\mathbf{P}^{\langle GS\rangle}\mathbf{T}_0^{\Omega(K,A_1)}\mathbf{P}^{\langle GS\rangle}$ denotes the projection of the operator $\mathbf{T}_0^{\Omega(K,A_1)}$. For simplicity, in all subsequent formulae, the same symbol will be used for one operator and its projections in all Hilbert subspaces. For instance, (7) will be rewritten as

$$\mathbf{H}^{\langle GS\rangle} = \sum \mathbf{t}_0^{\Omega(K,A_1)}\mathbf{T}_0^{\Omega(K,A_1)}. \tag{8}$$

Its matrix representation can be denoted by $\mathbf{H}^{\langle GS\rangle} = \mathbf{H}_{\{GS\}}^{\langle GS\rangle}$.

The effective Hamiltonian for the fundamental state $\langle\nu_s\rangle \equiv \{v_s = 1\}$ contains terms from $\widetilde{\mathbf{H}}_{\{GS\}}$ and $\widetilde{\mathbf{H}}_{\{\nu_s\}}$ only:

$$\begin{aligned} \mathbf{H}^{\langle\nu_s\rangle} &= \mathbf{P}^{\langle\nu_s\rangle}\left(\widetilde{\mathbf{H}}_{\{GS\}} + \widetilde{\mathbf{H}}_{\{\nu_s\}}\right)\mathbf{P}^{\langle\nu_s\rangle} \\ &= \sum \mathbf{t}_0^{\Omega(K,A_1)}\,\mathbf{T}_0^{\Omega(K,A_1)} + \sum \mathbf{t}_{s,s}^{\Omega(K,\Gamma)}\,\mathbf{T}_{s,s}^{\Omega(K,\Gamma)}. \end{aligned} \tag{9}$$

Its matrix representation can be expressed as the sum of two terms:

$$\mathbf{H}^{\langle\nu_s\rangle} = \mathbf{H}_{\{GS\}}^{\langle\nu_s\rangle} + \mathbf{H}_{\{\nu_s\}}^{\langle\nu_s\rangle}. \tag{10}$$

The effective Hamiltonian for the combination state $\langle\nu_s + \nu_{s'}\rangle \equiv \{v_s = v_{s'} = 1\}$ contains terms from $\widetilde{\mathbf{H}}_{\{GS\}}$, $\widetilde{\mathbf{H}}_{\{\nu_s\}}$, $\widetilde{\mathbf{H}}_{\{\nu_{s'}\}}$ and $\widetilde{\mathbf{H}}_{\{\nu_s+\nu_{s'}\}}$ only:

$$\begin{aligned} &\mathbf{H}^{\langle\nu_s+\nu_{s'}\rangle} = \\ &\mathbf{P}^{\langle\nu_s+\nu_{s'}\rangle}(\widetilde{\mathbf{H}}_{\{GS\}} + \widetilde{\mathbf{H}}_{\{\nu_s\}} + \widetilde{\mathbf{H}}_{\{\nu_{s'}\}} + \widetilde{\mathbf{H}}_{\{\nu_s+\nu_{s'}\}})\mathbf{P}^{\langle\nu_s+\nu_{s'}\rangle} \\ &= \sum \mathbf{t}_0^{\Omega(K,A_1)}\,\mathbf{T}_0^{\Omega(K,A_1)} + \sum \mathbf{t}_{s,s}^{\Omega(K,\Gamma)}\,\mathbf{T}_{s,s}^{\Omega(K,\Gamma)} \\ &+ \sum \mathbf{t}_{s',s'}^{\Omega(K,\Gamma)}\,\mathbf{T}_{s',s'}^{\Omega(K,\Gamma)} + \sum \mathbf{t}_{s,s'}^{\Omega(K,\Gamma)\Gamma_1\Gamma_2}\,\mathbf{T}_{s,s'}^{\Omega(K,\Gamma)\Gamma_1\Gamma_2}. \end{aligned} \tag{11}$$

Its matrix representation can be expressed as sum of four terms:

$$\begin{aligned} \mathbf{H}^{\langle\nu_s+\nu_{s'}\rangle} &= \mathbf{H}_{\{GS\}}^{\langle\nu_s+\nu_{s'}\rangle} + \mathbf{H}_{\{\nu_s\}}^{\langle\nu_s+\nu_{s'}\rangle} \\ &+ \mathbf{H}_{\{\nu_{s'}\}}^{\langle\nu_s+\nu_{s'}\rangle} + \mathbf{H}_{\{\nu_s+\nu_{s'}\}}^{\langle\nu_s+\nu_{s'}\rangle}. \end{aligned} \tag{12}$$

The effective Hamiltonian for the harmonic state $\langle 2\nu_s\rangle \equiv \{v_s = 2\}$ is similarly obtained by setting $s = s'$ in the above expression. Its matrix representation can be expressed as a sum of three terms:

$$\mathbf{H}^{\langle 2\nu_s\rangle} = \mathbf{H}_{\{GS\}}^{\langle 2\nu_s\rangle} + \mathbf{H}_{\{\nu_s\}}^{\langle 2\nu_s\rangle} + \mathbf{H}_{\{2\nu_s\}}^{\langle 2\nu_s\rangle}. \tag{13}$$

In the general notation $\mathbf{H}_{\{p\}}^{\langle P\rangle}$, $\langle P\rangle$ specifies the Hilbert subspace (associated to the polyad P) on which H is operating, whereas $\{p\}$ specifies the type of the vibrational operators involved (relating to the polyad p). The v quantum numbers of the states included in polyad p are less or equal

to that included in the polyad P. In practice, according to the so-called vibrational extrapolation scheme, the parameters involved in all subsequent effective Hamiltonian $\mathbf{H}^{\langle P\rangle}$ are those of the unique transformed Hamiltonian $\widetilde{\mathbf{H}}$ In the cases considered in this work, three types of parameters can be distinguished:

$\mathbf{t}_0^{\Omega(K,A_1)}$ so-called ground-state parameters;

$\mathbf{t}_{s,s}^{\Omega(K,\Gamma)}$ so-called ν_s parameters;

$\mathbf{t}_{ss',ss'}^{\Omega(K,\Gamma)\Gamma_1\Gamma_2}$ so-called $(\nu_s+\nu_{s'})$ parameters (or $2\nu_s$ parameters if $s=s'$).

Perevalov *et al.* [32–35] showed that different unitary transformations of the effective Hamiltonian can be considered. These transformations change the eigenfunctions of the Hamiltonian but do not change its eigenvalues:

$$\begin{aligned}\widetilde{\widetilde{\mathbf{H}}} &= \mathrm{e}^{\mathrm{i}S}\widetilde{\mathbf{H}}\mathrm{e}^{-\mathrm{i}S} \\ &= \sum \widetilde{\mathbf{t}}_{s\ldots,s'\ldots}^{\Omega(K,n\Gamma)\Gamma_1\Gamma_2} \times \mathbf{T}_{s\ldots,s'\ldots}^{\Omega(K,n\Gamma)\Gamma_1\Gamma_2} \end{aligned} \quad (14)$$

with

$$\mathbf{S} = \sum \mathbf{S}_{s\ldots,s'\ldots}^{\Omega(K,n\Gamma)\Gamma_1\Gamma_2} \left(\mathbf{R}^{\Omega(K,\Gamma)} \times {}^{\varepsilon}\mathbf{V}_{s\ldots,s'\ldots}^{\Gamma_1\Gamma_2(\Gamma)}\right)^{(A_1)}. \quad (15)$$

These transformations keep the operator form and eigenvalues unalterated but change the values of its parameters, according to:

$$\widetilde{\mathbf{t}} = \mathbf{t} + \Delta\mathbf{t}\left(s^{(1)}, s^{(2)}, \ldots\right). \quad (16)$$

Most of the $\mathbf{t}_{s\ldots,s'\ldots}^{\Omega(K,n\Gamma)\Gamma_1\Gamma_2}$ terms cannot be determined from observed lines in a unique way (for details, see Refs. [32–36]), they are not spectroscopic constants.

4 Data analysis

A new set of programs, grouped in a software package named STDS (Spherical Top Data System), was developed in the LPUB in Dijon [37]. These programs may be used to study the vibrational polyads with $J < 200$, they were adapted to refine at the same time several types of vibrational parameters that can belongs to the ground state, dyad states, hot band states, etc.; by fitting simultaneously several types of experimental data. The whole package STDS is freely accessible through ftp (user anonymous) at `jupiter.u-bourgogne.fr` or through the World Wide Web site at `fttp://www.u-bourgogne.fr/LPUB/STDS.html`.

The analysis is based on an iterative-weighted least squares fitting procedure of the transition wavenumbers. In order to minimize a dimensionless Q number in the least squares procedure, the weight w_i for each piece of data f_i is equal to the inverse of the square of the estimated uncertainty Δ_i:

$$Q = \sum_i \frac{\left(f_i^{\mathrm{obs}} - f_i^{\mathrm{cal}}\right)^2}{\Delta_i^2}. \quad (17)$$

In practice, we assigned an uncertainty Δ_i of 1×10^{-3} cm^{-1} to unblended transitions for the bending triad and of 0.3×10^{-3} cm^{-1} for the hot band bending triad minus bending dyad transitions.

The analysis of the bending triad [2] enabled us to assign 163 observed lines to hot band transitions up to $J = 9$. 135 presumably unblended lines were combined to infrared data corresponding to the bending triad to

Table 1. Hamiltonian parameters of the $2\nu_2$ and $(\nu_2+\nu_4)$ bands of $^{116}SnH_4$.

$\Omega(K,n\Gamma)$	$s_1s_2\Gamma_1s_3s_4\Gamma_2$	Value (cm^{-1})*
0(0, 0A1)	0200A1 0200A1	$-8.395(26)\times10^{-1}$
2(0, 0A1)	0200A1 0200A1	$1.121(22)\times10^{-3}$
0(0, 0A1)	0200 E 0200 E	1.32550(62)
2(0, 0A1)	0200 E 0200 E	$-9.86(76)\times10^{-5}$
1(1, 0F1)	2000A1 0101F1	$-4.237(24)\times10^{-2}$
1(1, 0F1)	0200 E 0101F1	$4.060(28)\times10^{-2}$
1(1, 0F1)	0200 E 0101F2	$-1.74(87)\times10^{-4}$
0(0, 0A1)	0200A1 0002A1	$-3.17(55)\times10^{-2}$
2(0, 0A1)	0200A1 0002A1	$6.17(66)\times10^{-4}$
0(0, 0A1)	0200 E 0002 E	$4.71(34)\times10^{-2}$
2(0, 0A1)	0200 E 0002 E	$-2.024(76)\times10^{-3}$
1(1, 0F1)	0200 E 0002F2	$7.389(97)\times10^{-2}$
0(0, 0A1)	0101F1 0101F1	2.30605(23)
1(1, 0F1)	0101F1 0101F1	$-4.589(10)\times10^{-2}$
2(0, 0A1)	0101F1 0101F1	$-1.1630(74)\times10^{-3}$
1(1, 0F1)	0101F1 0101F2	$-1.24941(49)\times10^{-1}$
0(0, 0A1)	0101F2 0101F2	$-7.6(1.1)\times10^{-4}$
1(1, 0F1)	0101F2 0101F2	$-3.39699(73)\times10^{-1}$
2(0, 0A1)	0101F2 0101F2	$-1.636(31)\times10^{-4}$
1(1, 0F1)	0101F1 0002A1	$1.0544(49)\times10^{-1}$
1(1, 0F1)	0101F1 0002 E	$-2.5247(51)\times10^{-1}$
1(1, 0F1)	0101F1 0002F2	$-1.7923(41)\times10^{-1}$
1(1, 0F1)	0101F2 0002 E	$-2.6628(47)\times10^{-1}$
0(0, 0A1)	0101F2 0002F2	$-8.5484(47)\times10^{-1}$
1(1, 0F1)	0101F2 0002F2	$1.4166(18)\times10^{-1}$
2(0, 0A1)	0101F2 0002F2	$1.040(12)\times10^{-3}$

*One standard deviation in paranthesis.

Table 2. Statistics on the fit of the hot band infrared transitions of $^{116}SnH_4$.

10 data for the (0200) ← (0100) band.

J	number of data	cumulated number of data	standard deviation (10^{-3} cm^{-1})	cumulated St. Dev. (10^{-3} cm^{-1})
6	2	2	0.310	0.310
7	3	5	0.709	0.583
8	3	8	0.403	0.523
9	2	10	0.098	0.470

124 data for the (0101) ← (0100) band.

J	number of data	cumulated number of data	standard deviation (10^{-3} cm^{-1})	cumulated St. Dev. (10^{-3} cm^{-1})
0	1	1	0.839	0.839
1	6	7	0.717	0.736
2	9	16	0.532	0.629
3	12	28	0.713	0.667
4	14	42	0.756	0.697
5	17	59	0.773	0.720
6	17	76	0.549	0.687
7	17	93	0.649	0.680
8	18	111	0.803	0.702
9	13	124	0.666	0.698

1 data for the (0101) ← (0001).

J	number of data	cumulated number of data	standard deviation (10^{-3} cm^{-1})	cumulated St. Dev. (10^{-3} cm^{-1})
7	1	1	0.244	0.244

determine the Hamiltonian parameters. The simultaneous analysis of these data enabled us to determine 26 parameters for the two bands $2\nu_2$ and $(\nu_2+\nu_4)$, using a Hamiltonian developed to the fourth order (Tab. 1). The RMS for the hot band transitions used in the fit was about 2.26×10^{-3} cm^{-1} while the standards deviation for the fit of the parameters was 1.5×10^{-3} cm^{-1}. Statistics of the fit are listed in Table 2. Table 3 regroups the assignments made for the hot band transitions with the difference between observed and calculated frequencies.

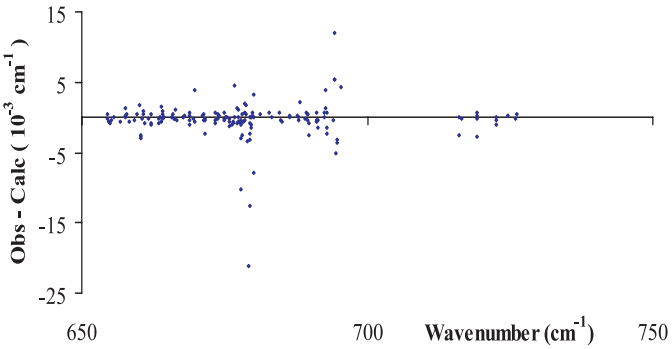

Fig. 2. Obs-Calc residuals as a function of the wavenumber.

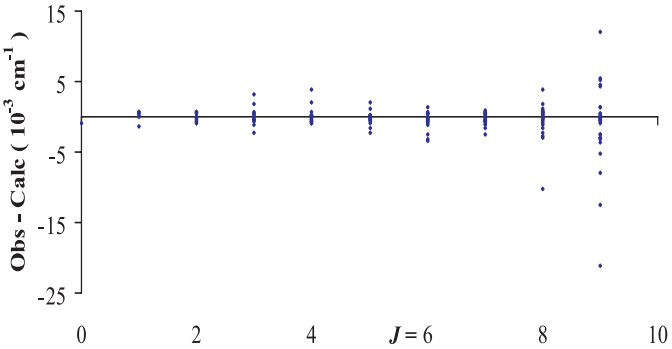

Fig. 3. Obs-Calc residuals as a function of the rotational J number.

5 Discussion

It's well-known that the $2\nu_2$, $(\nu_2+\nu_4)$ and the $2\nu_4$ bands of the bending triad are perturbed by resonance interaction. However, for relatively low values of J ($J<10$) the isolated-state model is still applicable. As the line intensity of vibrational levels of the $2\nu_4$ band is small, it was so difficult for us to assign the transitions corresponding to this band. Thus, in the aim to minimize the resonance interaction effect between the $(\nu_2+\nu_4)$ and $2\nu_4$ bands, we analysed the infrared spectra up to $J=9$. Figure 2 shows the Obs-Calc residuals plotted as a function of the wavenumber and Figure 3 shows them as a function of the rotational J number. This emphasizes the effect of neglected perturbations that increases as J value. One can see that the calculations for the hot band transitions are in good agreement with experimental data (Tab. 3). The set of parameters determined for the two bands $2\nu_2$ and $(\nu_2+\nu_4)$ can be used to analyse completely the bending triad using a spectrum more intense in this region and with help of the hot band transitions assignments.

The author A. Tabyaoui would like to thank Ch. Wenger for his invaluable assistance. The "*Conseil Régional de Bourgogne*" is gratefully acknowledged for the financial support to the "*Laboratoire de Physique de l'Université de Bourgogne*".

Table 3. Assignments of the hot band infrared transitions of $^{116}SnH_4$.

Obs (cm^{-1})	Calc (cm^{-1})	Obs–Calc (10^{-3} cm^{-1})	Assignments					
654.5296	654.5297	−0.1124	10	F1	11	9	F2	24
654.5437	654.5433	0.3650	10	A1	4	9	A2	9
654.6731	654.6737	−0.5294	10	F2	11	9	F1	25
654.8776	654.8785	−0.8839	10	A2	4	9	A1	8
655.2688	655.2691	−0.3737	10	F2	13	9	F1	28
655.5852	655.5851	0.0939	10	E	9	9	E	18
656.8451	656.8456	−0.5257	10	F1	13	9	F2	27
657.6139	657.6126	1.3131	10	F2	12	9	F1	29
657.6763	657.6761	0.2029	9	F1	10	8	F2	22
657.7052	657.7051	0.0573	9	E	7	8	E	15
657.9287	657.9283	0.3990	9	F2	10	8	F1	21
658.3189	658.3196	−0.6169	9	F1	11	8	F2	25
659.2121	659.2124	−0.3089	9	E	8	8	E	17
659.5672	659.5666	0.5453	9	F2	11	8	F1	24
660.1022	660.1004	1.7537	9	A2	4	8	A1	9
660.2566	660.2596	−2.9483	10	E	8	9	E	19
660.3022	660.3051	−2.8574	10	F1	12	9	F2	28
660.3855	660.3881	−2.5479	10	A1	5	9	A2	10
660.6277	660.6278	−0.0878	8	F2	9	7	F1	20
660.7599	660.7594	0.4855	8	E	6	7	E	13
660.8899	660.8891	0.7888	8	F1	9	7	F2	19
661.0806	661.0814	−0.8360	8	A1	4	7	A2	8
661.6291	661.6292	−0.1213	8	F1	10	7	F2	22
662.0653	662.0648	0.4767	8	F2	10	7	F1	22
662.1077	662.1088	−1.1060	9	F2	12	8	F1	25
662.2349	662.2357	−0.8427	9	F1	12	8	F2	26
663.5039	663.5040	−0.1268	7	F2	8	6	F1	16
663.5922	663.5930	−0.7808	7	A2	3	6	A1	7
663.6136	663.6136	−0.0148	7	F1	8	6	F2	17
663.8588	663.8594	−0.6139	8	A2	4	7	A1	7
663.8752	663.8737	1.4702	7	A1	3	6	A2	6
664.0518	664.0510	0.8384	8	F2	11	7	F1	23
664.1256	664.1253	0.3587	8	E	7		E	15
664.1361	664.1364	−0.2809	7	F1	9	6	F2	19
664.3570	664.3571	−0.0602	7	E	6	6	E	13
665.8020	665.8020	−0.0152	7	F2	9	6	F1	19
666.0112	666.0108	0.3934	7	F1	10	6	F2	20
666.1770	666.1772	−0.1177	6	E	5	5	E	9
666.2728	666.2730	−0.1491	6	F2	7	5	F1	15
666.3897	666.3885	1.1768	6	F1	7	5	F2	14
666.5938	666.5943	−0.4424	6	F2	8	5	F1	17
667.6507	667.6507	−0.0177	6	E	6	5	E	11
667.7773	667.7772	0.1163	6	F1	8	5	F2	16
667.9616	667.9614	0.1695	6	A1	3	5	A2	6
668.8250	668.8247	0.3264	5	F2	6	4	F1	11
668.8250	668.8242	0.7565	5	E	4	4	E	9
668.8290	668.8300	−1.0147	5	F1	6	4	F2	12

Table 3. *Continued.*

Obs (cm^{-1})	Calc (cm^{-1})	Obs–Calc (10^{-3} cm^{-1})	Assignments					
668.8607	668.8611	−0.4011	5	A2	3	4	A1	5
669.5131	669.5132	−0.1292	5	F2	7	4	F1	13
669.6829	669.6789	3.9180	5	A1	2	4	A2	4
669.7277	669.7283	−0.5829	5	F1	7	4	F2	14
671.1460	671.1458	0.2586	4	F2	5	3	F1	10
671.2460	671.2464	−0.4015	4	F1	5	3	F2	9
671.4066	671.4061	0.4762	4	A2	2	3	A1	3
671.4759	671.4762	−0.2546	4	F2	6	3	F1	11
671.5844	671.5848	−0.4487	4	E	4	3	E	7
671.6278	671.6301	−2.3304	4	A1	2	3	A2	4
673.3956	673.3964	−0.7304	3	F1	5	2	F2	8
673.4523	673.4517	0.5904	3	E	3	2	E	5
673.4553	673.4558	−0.4739	3	F2	4	2	F1	6
673.8574	673.8576	−0.2273	3	F1	4	2	F2	7
673.9106	673.9102	0.3877	9	F2	8	9	F1	20
673.9935	673.9933	0.1886	9	F1	8	9	F2	19
674.8838	674.8839	−0.1228	8	E	5	8	E	12
674.9227	674.9220	0.6953	2	A1	2	1	A2	2
674.9452	674.9456	−0.3565	8	F1	7	8	F2	18
675.0845	675.0845	0.0299	8	A1	3	8	A2	6
675.3440	675.3439	0.0533	2	F1	3	1	F2	4
675.7386	675.7392	−0.6199	7	F2	6	7	F1	16
675.8323	675.8336	−1.3173	2	E	2	1	E	3
675.9326	675.9329	−0.2066	7	F1	7	7	F2	15
676.3727	676.3738	−1.1193	6	A2	2	6	A1	6
676.4718	676.4726	−0.8391	1	F1	2	0	F2	2
676.5989	676.5995	−0.5499	6	F2	6	6	F1	13
676.7378	676.7332	4.6244	9	A1	3	9	A2	8
676.7408	676.7407	0.0377	6	E	4	6	E	9
677.0906	677.0892	1.3398	9	F1	9	9	F2	20
677.1022	677.1030	−0.7311	5	F2	5	5	F1	12
677.3570	677.3576	−0.5759	9	E	6	9	E	13
677.4258	677.4258	−0.0036	5	F1	5	5	F2	11
677.5252	677.5242	0.9914	8	F1	8	8	F2	19
677.5824	677.5831	−0.6579	4	E	3	4	E	7
677.7834	677.7839	−0.4295	4	F1	4	4	F2	10
677.8112	677.8214	−10.2436	8	A2	3	8	A1	7
677.8175	677.8205	−2.9768	8	F2	8	8	F1	17
677.8624	677.8632	−0.8244	2	A2	1	2	A1	3
677.9282	677.9292	−1.0412	3	F2	3	3	F1	8
677.9819	677.9814	0.4553	7	E	5	7	E	11
678.1180	678.1205	−2.5292	7	F2	7	7	F1	17
678.3454	678.3461	−0.6579	6	F1	6	6	F2	14
678.5627	678.5607	2.0312	4	A1	2	4	A2	3
678.5728	678.5733	−0.5036	5	A1	2	5	A2	5
678.6429	678.6422	0.7279	1	F2	2	1	F1	4
678.7463	678.7459	0.4422	2	F2	3	2	F1	5

Table 3. *Continued.*

Obs (cm^{-1})	Calc (cm^{-1})	Obs–Calc (10^{-3} cm^{-1})	Assignments					
678.7840	678.7822	1.7212	3	F1	4	3	F2	7
679.0969	679.1002	−3.3326	6	E	5	6	E	10
679.2718	679.2929	−21.0773	9	E	7	9	E	14
679.3318	679.3327	−0.8691	5	F1	6	5	F2	12
679.3891	679.3914	−2.2769	5	F2	6	5	F1	13
679.4161	679.4192	−3.0972	6	F2	7	6	F1	14
679.4640	679.4638	0.1247	4	F1	5	4	F2	11
679.5159	679.5284	−12.5433	9	F2	10	9	F1	23
679.5597	679.5612	−1.5051	5	E	4	5	E	8
679.5860	679.5870	−0.9945	4	A2	2	4	A1	4
679.6137	679.6137	0.0033	4	F2	5	4	F1	9
679.6753	679.6752	0.0636	3	E	3	3	E	5
679.7959	679.7953	0.5668	3	F2	4	3	F1	9
679.9453	679.9450	0.2324	1	F1	2	1	F2	3
680.0417	680.0385	3.2128	3	F1	5	3	F2	8
680.0564	680.0643	−7.9507	9	F1	10	9	F2	22
680.0803	680.0802	0.1071	2	F1	3	2	F2	6
681.1905	681.1900	0.5281	0	E	1	1	E	2
682.8799	682.8792	0.7113	1	F1	2	2	F2	5
683.1731	683.1730	0.025	1	F2	2	2	F1	4
684.5837	684.5830	0.7196	2	F1	3	3	F2	6
684.7743	684.7746	−0.3812	2	E	2	3	E	4
685.0269	685.0274	−0.5877	2	F2	3	3	F1	7
686.3234	686.3232	0.1359	3	F2	4	4	F1	7
686.4463	686.4463	−0.0006	3	E	3	4	E	6
687.8439	687.8437	0.2198	4	E	4	5	E	6
687.9844	687.9843	0.0713	4	A2	2	5	A1	3
688.0429	688.0433	−0.3642	4	F2	5	5	F1	10
688.1460	688.1438	2.1085	4	F1	5	5	F2	9
689.0403	689.0405	−0.2314	4	E	3	5	E	7
689.4070	689.4063	0.7178	5	A2	3	6	A1	5
689.5121	689.5115	0.5342	5	F2	7	6	F1	12
689.5538	689.5532	0.5264	5	F1	7	6	F2	13
689.6250	689.6254	−0.3712	5	F2	6	6	F1	10
689.6961	689.6969	−0.854	5	E	4	6	E	8
689.7519	689.7544	−2.4606	5	F1	6	6	F2	11
691.1934	691.1940	−0.6339	6	E	6	7	E	10
691.2106	691.2100	0.5884	6	F1	7	7	F2	12
691.2197	691.2202	−0.4805	6	F1	8	7	F2	14
691.2635	691.2638	−0.3495	6	A1	3	7	A2	5
691.3095	691.3110	−1.5560	6	F2	7	7	F1	13
692.5395	692.5395	0.0254	7	F1	9	8	F2	16
692.5669	692.5663	0.6198	7	E	6	8	E	11
692.7186	692.7174	1.2090	7	F1	8	8	F2	14
692.7615	692.7576	3.9614	7	A1	3	8	A2	5
692.8849	692.8872	−2.3530	7	F2	9	8	F1	16
692.8904	692.8898	0.5779	7	A2	3	8	A1	6

Table 3. *Continued.*

Obs (cm^{-1})	Calc (cm^{-1})	Obs–Calc (10^{-3} cm^{-1})	Assignments					
692.9361	692.9376	−1.5226	7	F1	10	8	F2	17
693.9935	693.9938	−0.2977	8	A1	4	9	A2	7
694.2150	694.2029	12.0247	8	F1	9	9	F2	15
694.2414	694.2360	5.3441	8	F2	9	9	F1	16
694.2468	694.2415	5.3199	8	E	6	9	E	10
694.5634	694.5686	−5.1996	8	A2	4	9	A1	6
694.6120	694.6157	−3.6570	8	F2	11	9	F1	19
694.6319	694.6350	−3.1246	8	E	7	9	E	12
695.3501	695.3457	4.3705	8	F1	8	9	F2	16
716.0510	716.0536	−2.6064	10	F2	13	9	F1	37
716.0786	716.0785	0.0746	10	F1	13	9	F2	35
716.5453	716.5454	−0.1174	10	F2	10	9	F1	34
719.1787	719.1815	−2.8326	9	F1	11	8	F2	32
719.2676	719.2670	0.5931	9	A2	4	8	A1	12
719.2676	719.2678	−0.2622	9	E	8	8	E	22
719.2676	719.2673	0.2604	9	F2	11	8	F1	31
722.4808	722.4820	−1.1440	8	A1	4	7	A2	10
722.5576	722.5581	−0.4443	8	F1	10	7	F2	28
722.5819	722.5818	0.0164	8	F2	10	7	F1	29
724.7180	724.7178	0.2442	8	F2	1	7	F1	15
726.0105	726.0107	−0.2024	7	F1	9	6	F2	25
726.2777	726.2773	0.3892	7	A2	3	6	A1	9

References

1. F. Brunet, G. Pierre, H. Bürger, J. Mol. Spectrosc. **140**, 237 (1990)
2. A. Tabyaoui, G. Pierre, H. Bürger (in preparation)
3. I.W. Levin, H. Ziffer, J. Chem. Phys. **43**, 4023 (1965)
4. I.W. Kattenberg, A. Oskam, J. Mol. Spectrosc. **51**, 377 (1974)
5. F.W. Birss, Mol. Phys. **31**, 491 (1976)
6. A. Cabana *et al.*, Mol. Phys. **36**, 1503 (1978)
7. P. Lepage, J.P. Champion, A.G. Robiette, J. Mol. Spectrosc. **89**, 440 (1981)
8. M. Mizushima, P. Venkateswarlu, J. Chem. Phys. **21**, 705 (1953)
9. I.M. Mills, J.K.G. Watson, W.L. Smith, Mol. Phys. **16**, 329 (1969)
10. M. Oldani *et al.*, J. Mol. Spectrosc. **113**, 229 (1985)
11. M. Oldani, A. Bauder, G. Pierre, J. Mol. Spectrosc. **117**, 435 (1986)
12. M. Takami, J. Chem. Phys. **71**, 4164 (1979)
13. M. Takami, J. Chem. Phys. **73**, 2665 (1980)
14. M. Takami, J. Chem. Phys. **74**, 4276 (1981)
15. M. Takami, J. Chem. Phys. **76**, 1670 (1982)
16. M. Takami, J. Mol. Spectrosc. **93**, 250 (1982)
17. L. Jörissen *et al.*, J. Chem. Phys. **90**, 2109 (1989)
18. S.M. Kirschner, J.K.G. Watson, J. Mol. Spectrosc. **47**, 347 (1973)
19. A.G. Robiette, D.L. Gray, F.W. Birss, Mol. Phys. **32**, 1591 (1976)
20. J. Susskind, J. Chem. Phys. **56**, 5152 (1972)
21. Y. Ohshima *et al.*, J. Chem. Phys. **85**, 5519 (1986)
22. Y. Ohshima *et al.*, J. Chem. Phys. **87**, 5141 (1987)
23. V.M. Krivtsun *et al.*, J. Mol. Spectrosc. **139**, 107 (1990)
24. A. Tabyaoui *et al.*, Phys. Chem. News **10**, 106 (2003)
25. A. Tabyaoui *et al.*, J. Mol. Spectrosc. **148**, 100 (1991)
26. M. Halonen *et al.*, J. Chem. Phys. **93**, 1607 (1990)
27. M. Halonen, L. Halonen, J. Chem. Phys. **108**, 9285 (1998)
28. G. Guelachvili, K. Narahari Rao, *Handbook of Infrared Standards* (Academic Press, San Diego, 1986)
29. J.P. Champion, Can. J. Phys. **55**, 1802 (1977)
30. J.P. Champion, G. Pierre, J. Mol. Spectrosc. **79**, 255 (1980)
31. J.P. Champion, M. Loëte, G. Pierre, in *Spectroscopy of the earth's atmosphere and interstellar molecules*, edited by K.N. Rao, A. Weber (Academic Press, Inc. U.S.A., 1992), p. 339
32. V.I. Perevalov, V.G. Tyuterev, B.I. Zhilinskii, Dokl. Acad. Nauk SSSR **263**, 868 (1982)
33. V.I. Perevalov, V.G. Tyuterev, B.I. Zhilinskii, J. Mol. Spectrosc. **103**, 147 (1984)
34. V.I. Perevalov, V.G. Tyuterev, B.I. Zhilinskii, Chem. Phys. Lett. **104**, 455 (1984)
35. V.I. Perevalov, V.G. Tyuterev, B.I. Zhilinskii, J. Mol. Spectrosc. **111**, 1 (1985)
36. C. Pierre, M. Loëte, G. Pierre, Can. J. Phys. **65**, 708 (1987)
37. M. Rey *et al.*, J. Mol. Spectrosc. **219**, 313 (2003)